$(AGN)^2$

9. H II Regions in the Galactic Context

Week 13

May 20 (Monday), 2024

updated on 05/18, 19:44

선광일 (Kwangil Seon)

KASI / UST

9.2 Distribution of H II Regions in Other Galaxies

- The best spectral region to trace H II regions is the red, centered around Hα 6563 and [N II] $\lambda\lambda$6583, 6548.
  - Comparison with a narrow band image in the nearby continuum permits nearly complete discrimination between H II regions and continuum sources, which are apparently mostly luminous stars and small, luminous, star clusters.
- Surveys of H II regions
  - In our own Galaxy, the more distant parts are nearly completely inaccessible to optical observation because of strong extinction near the galactic plane.
  - Many external galaxies have been surveyed for H II regions in these ways. The entire galaxy can be observed. All parts of it are very nearly the same distance from the observer.
  - All the nearby, well-studied spiral galaxies contain may H II regions. On the other hand, elliptical and S0 galaxies typically do not contain H II regions.
  - In spiral galaxies, the H II regions are concentrated along the spiral arms. Often there are no H II regions in the inner parts of the spiral galaxies. However, the spiral arms in the inner regions can be traced as concentrated regions of extinction, but there is no O stars to ionize it.

- NASA/IPAC Extragalactic Database
  - https://ned.ipac.caltech.edu/

- NGC 4321
  - a nearly face-on spiral galaxy.
  - The left image was taken using a filter centered on Hα and [N II].
  - The right image was taken with a red continuum filter (R filter).

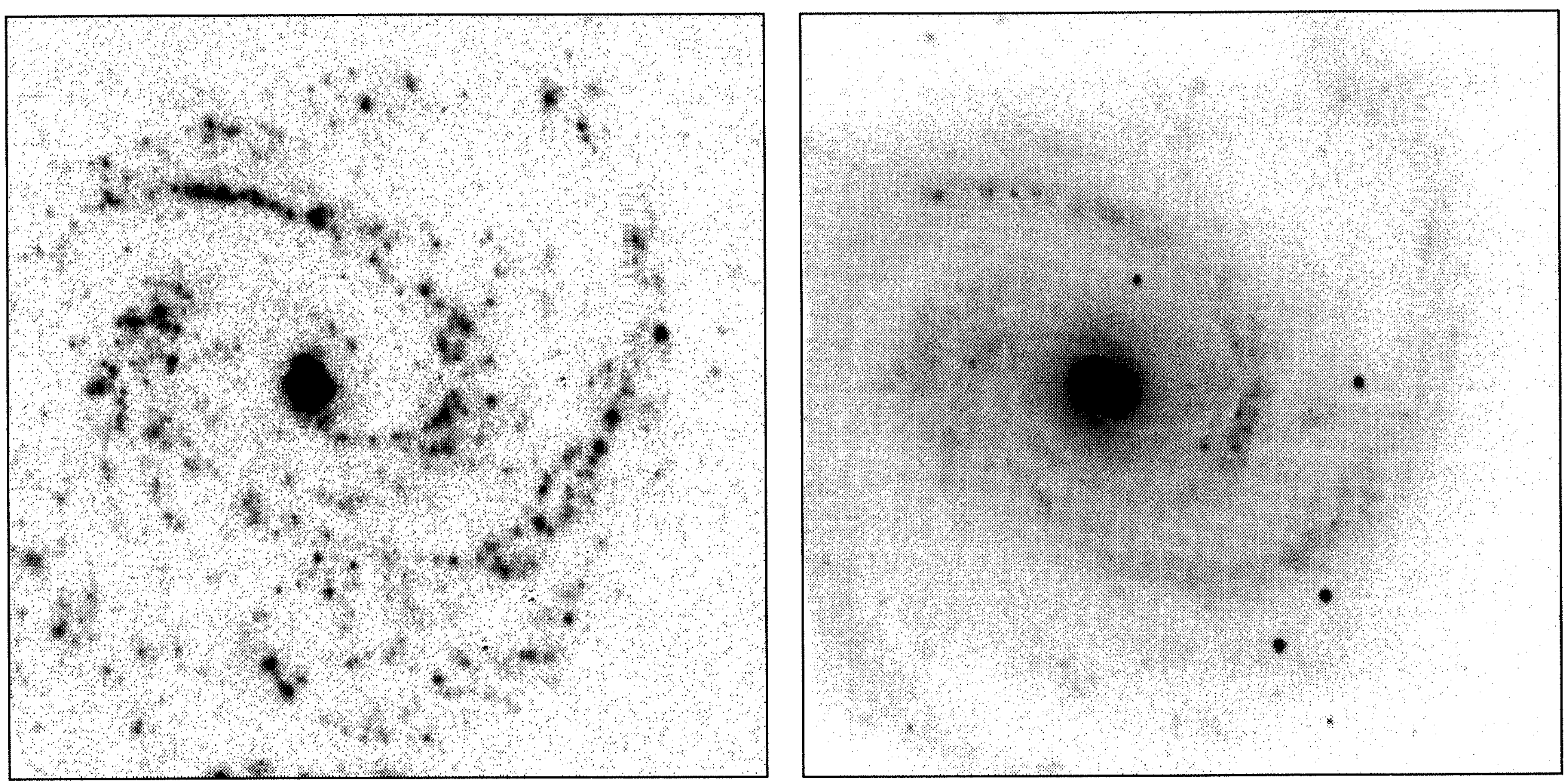

Figure 9.1

Irregular Galaxies

- In irregular galaxies, the distribution of H II regions is less well organized.
  - In LMC, features resembling spiral arms can be traced in the distribution of H II regions. (only one spiral arm)
  - But, in SMC, the distribution of H II regions is often far less symmetric.
- Some of these galaxies contain H II emission spread through much of their volume. These are called **H II galaxies**, extragalactic H II regions, or blue compact dwarf (BCD) galaxies.
  - A BCG galaxy is a small galaxy which contains large clusters of young, hot, massive stars. These stars, the brightest of which are blue, cause the galaxy itself to appear blue in color.

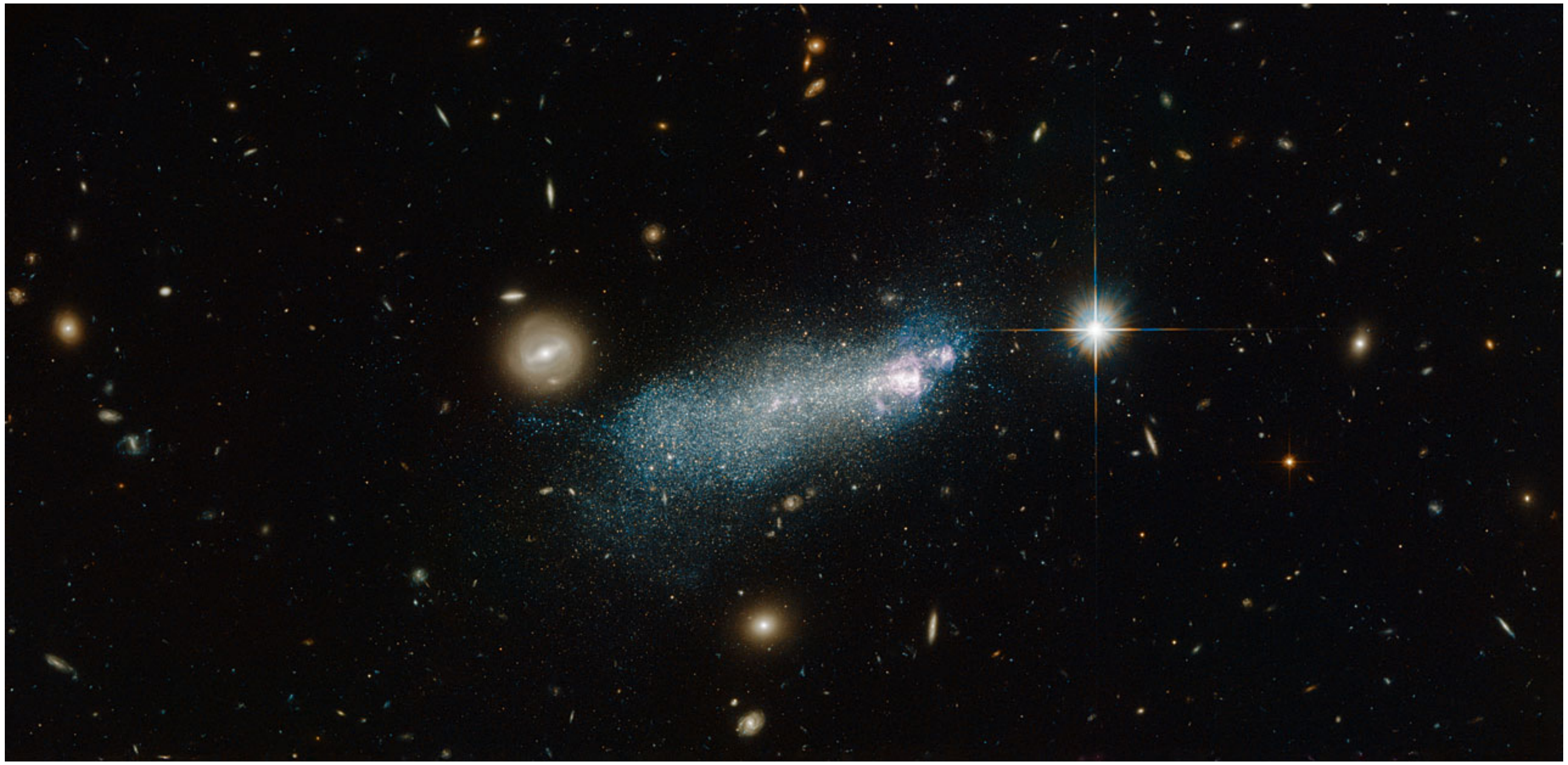

Blue compact dwarf PGC 51017
NASA/ESA HST image

9.3 Distribution of H II Regions in Our Galaxy

- Spatial distribution of H II regions
  - The H II regions in our Galaxy are also concentrated to spiral arms.
  - H II regions are strongly concentrated to the galactic plane because they are all close to the galactic equator in the sky.
  - However, our location and the strong concentration of interstellar dust to the galactic plane make it difficult to survey for H II regions and to determine their distances accurately.
- All sky Hα map
  - Composition of WHAM, VTSS, SHASSA survey (Finkbeiner 2003, ApJS)
  - https://lambda.gsfc.nasa.gov/product/foreground/fg_halpha_info.html
  - https://faun.rc.fas.harvard.edu/dfink/skymaps/halpha/

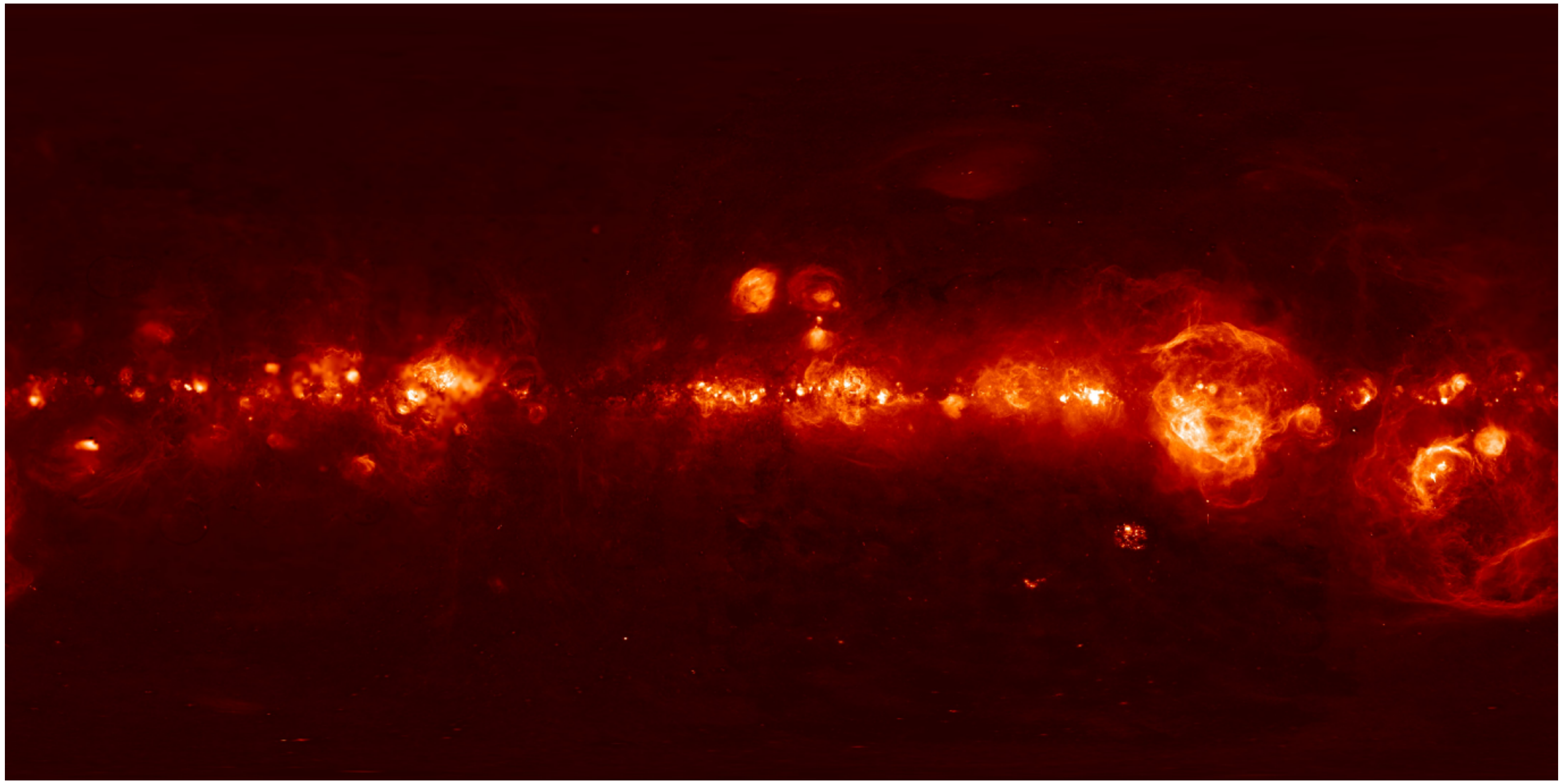

WHAM - Wisconsin H-Alpha Mapper
VTSS - Virginia Tech Spectral-Line Survey
SHASS - Southern H-alpha Sky Survey

- Distance & Spiral arms
  - Original method was to identify the exciting O star, classify their spectra, and find their distances from absolute magnitudes corrected for extinction from their measured colors.
  - If the cluster or association have several O stars or luminous B stars, each one provides an independent distance estimate (this reduces some of errors due to dispersion in absolute magnitude and intrinsic color)
  - Another approach to locating the spiral arms is to find the distances of numerous young galactic clusters, even if they do not contain O stars or have no observable H II region.
  - The UBV photometry and fitting to a standard zero-age main sequence are used to eliminate extinction and obtain the distance. This method is probably more accurate than the method using the spectral types of a few O stars and there are many more clusters.
- The structure of the spiral arms is best traced using MIR wavelengths beyond 2 μm, where the extinction is much smaller.
  - Next page show the spiral arms in our Galaxy, traced by the Spitzer Space Telescope & Gaia mission.

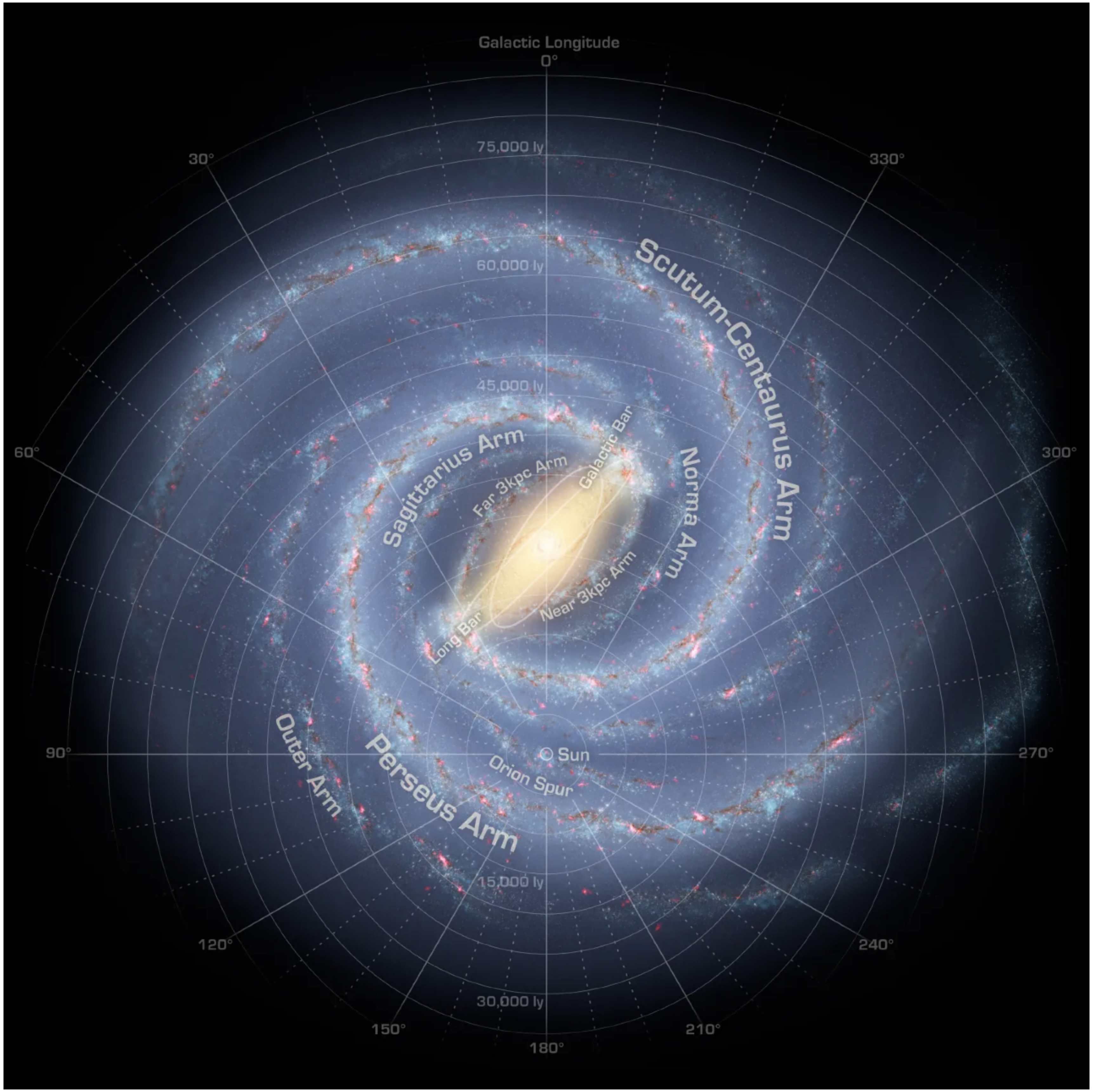

Our sun lines near a small, partial arm called the Orion Arm, or Orion Spur, located between the Sagittarius and Perseus arms.

The sun is located around 8.5 kpc away from the core of the Galaxy, and is rotating at a velocity of 220 km/s.

credit : NASA/JPL-Caltech/ R. Hurt (SSC/Caltech)

Figure 9.3

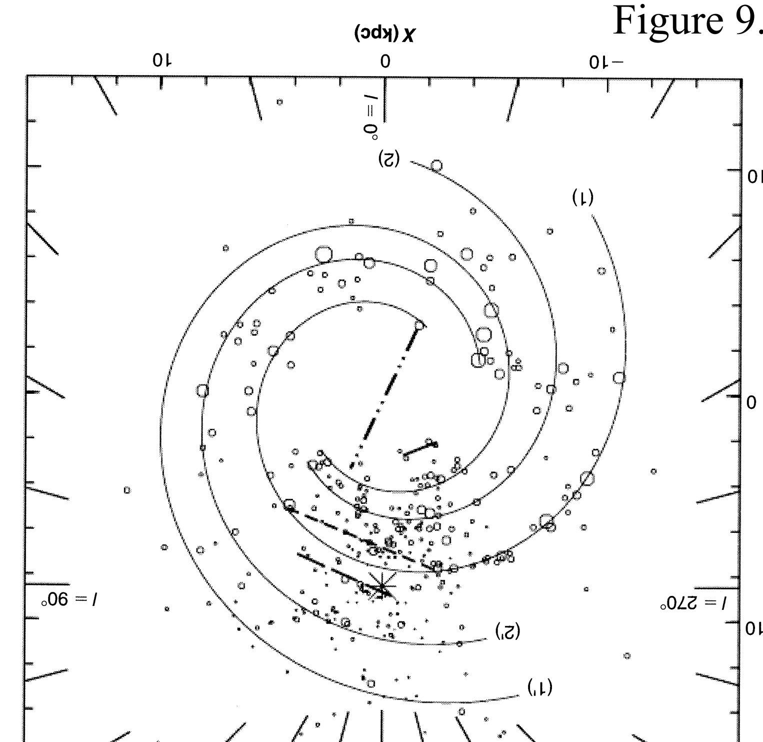

- Radio Observations
  - There is almost zero extinction in the radio-frequency region. Radial velocities can be measured with high accuracy for interstellar gas, which emits spectral line, such as H I λ21.1 cm.
  - If the variation of circular velocity with distance from the Galactic center is known, these radial velocities can be converted into distances.
  - Early maps of the spiral arms were obtained using neutral H^0. At present, much more accurate velocity measurements can be made by the sharper CO λ2.59 mm line in molecular clouds, or radio recombination lines such as H109α λ5.99 cm in H II regions.
- Our Galaxy is most likely to be an Sbc type (Hubble classification scheme).

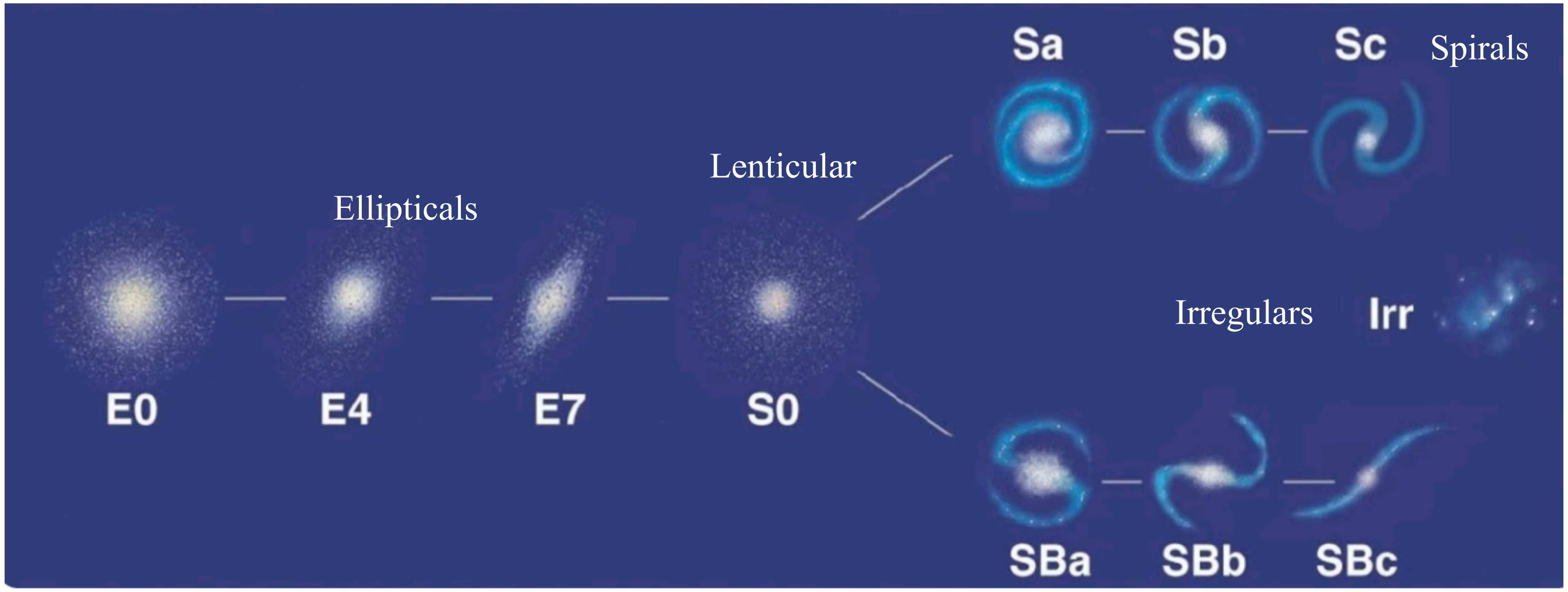

Sa: strong bulge and tight, indistinct arms
Sb: intermediate type
Sc: small bulge and loose, well-defined arms
Sd: no bulge and all sharp arms

B: barred galaxies

https://www.youtube.com/watch?v=jyAks7XTEfw&ab_channel=JasonKendall for the Hubble tuning fork

- Ambiguity in the Galactic rotation method
  - The galactic rotation model does not uniquely determine the distance of H II regions closer to the center of the Galaxy than the sun.
  - This ambiguity does not exist for H II regions more distant from the galactic center than the sun.

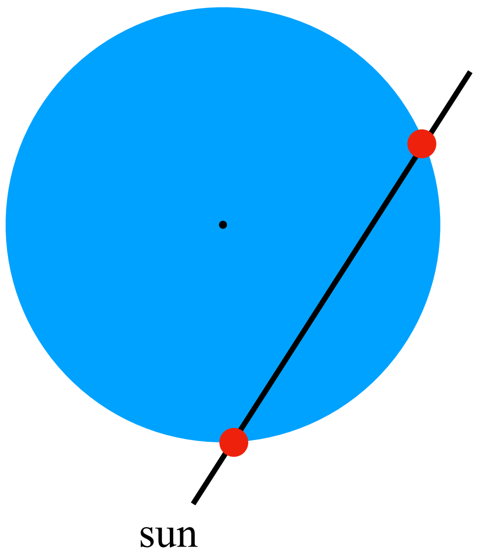

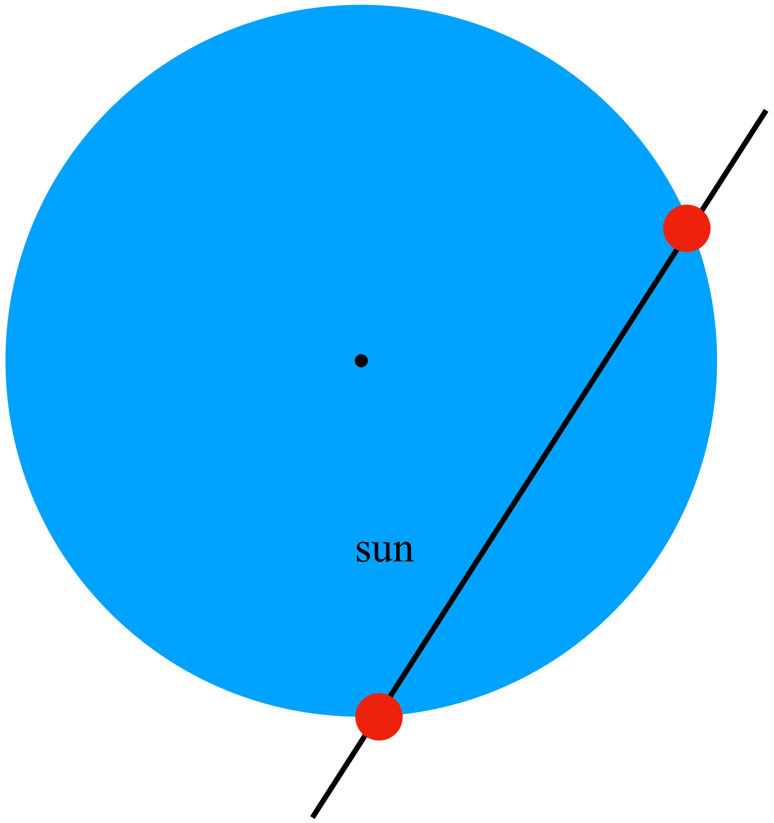

- Galaxies

credit: Jason Kendall

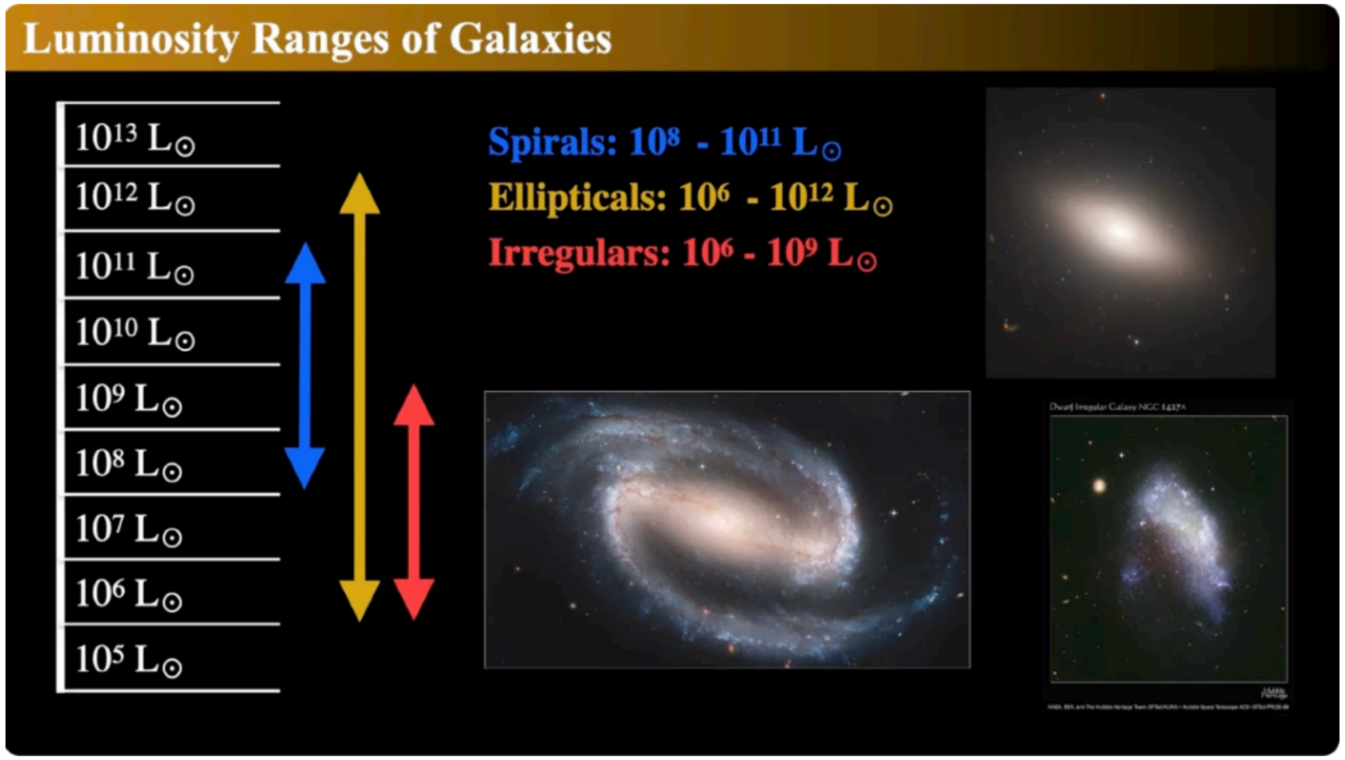

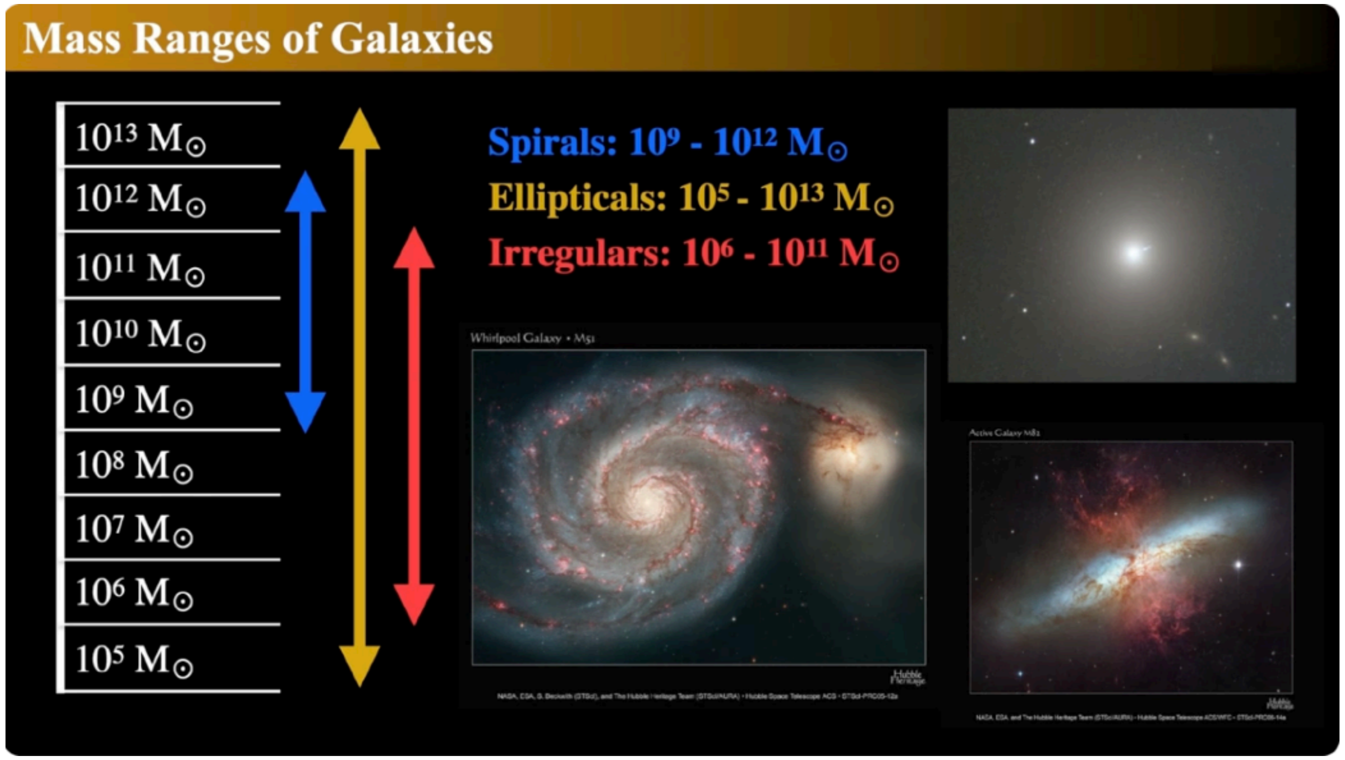

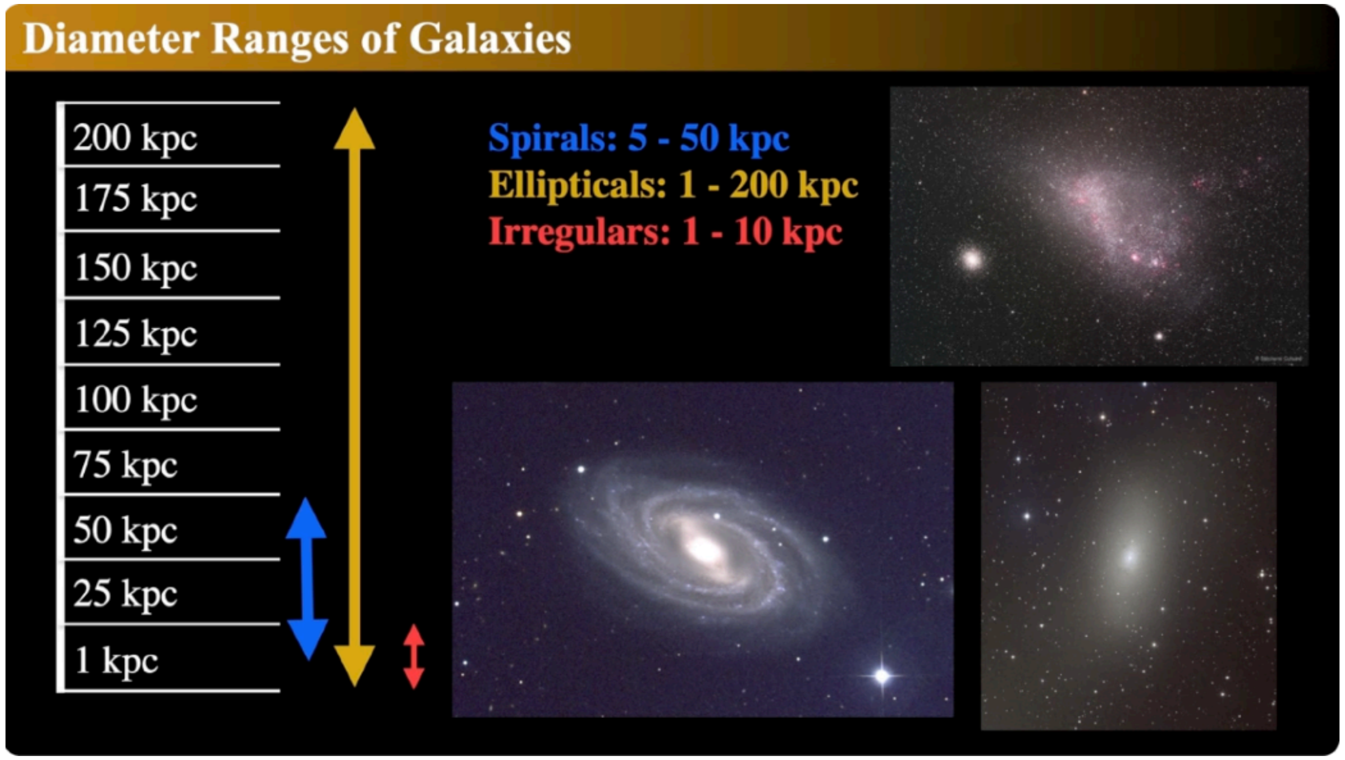

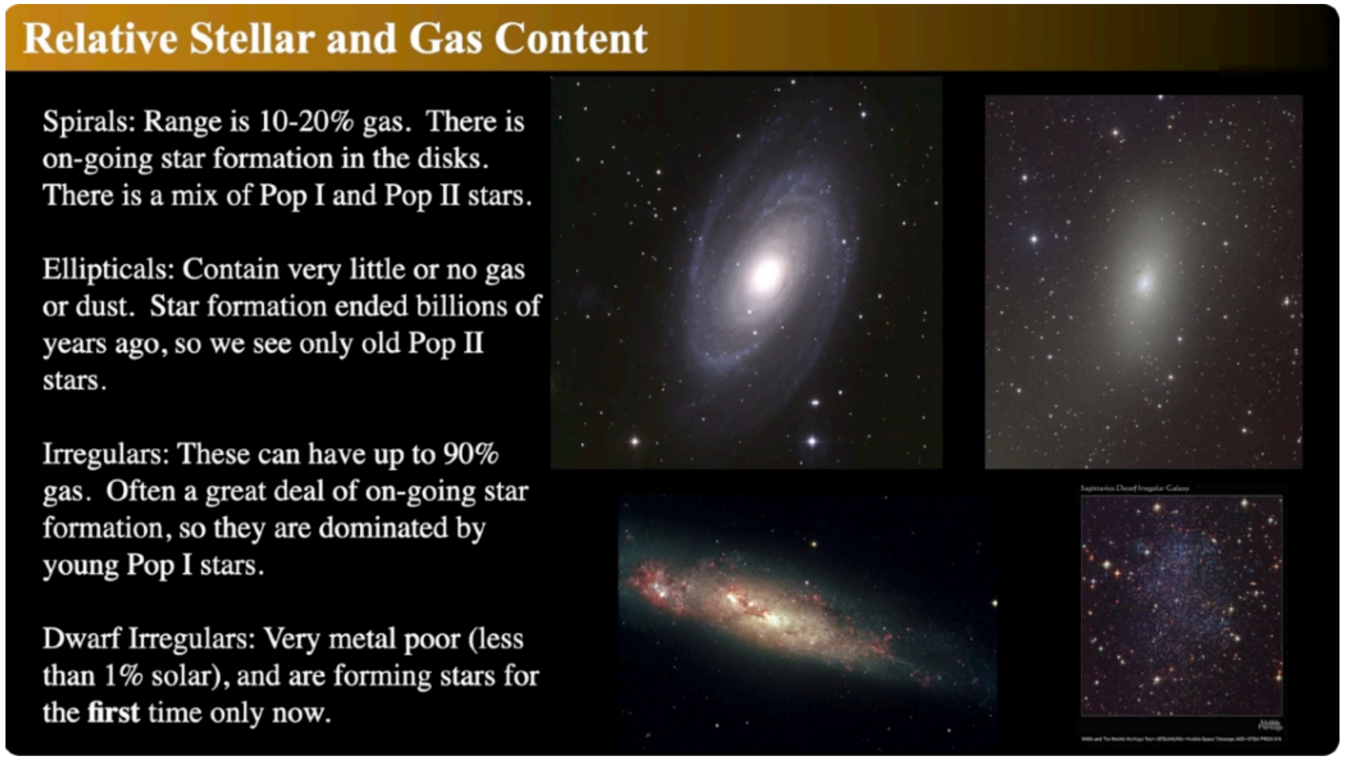

9.4 Stars in H II Regions

- The Hα luminosity is proportional to the number of hydrogen-ionizing photons radiated by the central star.
    - Orion Nebula is mainly ionized by a single O6 star.
    - The largest H II regions in our Galaxy and in other galaxies are ionized by clusters or associations of O stars rather than by a single star.
    - Orion Nebula-like H II regions are probably present in other galaxies, but they are too faint to have been well studied.

Hα luminosities and star formation rates

Object	$L(\mathrm{H}\alpha)$ (erg s^{-1})	$Q(\mathrm{H}^0)$ (s^{-1})	SFR ($M_\odot$ yr^{-1})
NGC 1976	5.0×10^{36}	3.7×10^{48}	3.9×10^{-5}
SMC	4.8×10^{39}	3.5×10^{51}	3.8×10^{-2}
LMC	2.7×10^{40}	2.0×10^{52}	2.1×10^{-1}
H237 (in M 101)	1.2×10^{39}	8.8×10^{50}	9.3×10^{-3}
NGC 5455 (in M 101)	1.1×10^{40}	8.0×10^{51}	8.3×10^{-2}
NGC 5461 (in M 101)	2.5×10^{40}	1.8×10^{52}	2.0×10^{-1}

- O stars have short lives, approximately 4×10^6 years, for an O6 star.
    - Therefore, they all formed recently.
    - There are also many less luminous stars, and they also formed recently.
    - Stars over a wide range of luminosity, or mass, have formed recently there.

- Initial Mass Function
  - We assume star formation occurs with a range of masses given by an initial mass function, or ISM.
    - Star formation occurs when an interstellar cloud undergoes gravitational collapse. It fragments into a large number of smaller clumps, eventually form stars with masses in the range $10^{-1}M_\odot \le M \le 10^2 M_\odot$.
    - The IMF gives the number of stars per unit mass interval,

$$\varphi(M) \propto \frac{dN}{dM}.$$

    - The form of $\varphi(M)$ is derived from the observational data for the distribution of stars of various masses in the "solar vicinity" (within 2 kpc).
  - Salpeter IMF (1955)
    - The observed population must be corrected for the fact that more massive stars are short-lived, and so are under represented compared to longer-lived stars. Most detailed studies have found that the normalized IMF can be represented by

$$M\varphi(M) = 0.17M^{-1.35} \quad \rightarrow \quad \int_{0.1M_\odot}^{100M_\odot} M\varphi(M)dM = 1 \qquad \text{or} \qquad \varphi(M)dM \propto M^{-2.35}dM$$

    - This indicates that the newly-formed stellar population is weighted towards smaller masses. It must be kept in mind that this IMF may not be applicable to other regions, galaxies, and times.

- Kroupa IMF (2001, 2002)

$$\begin{aligned}\varphi(M) &= Ak_0 M^{-0.3} \quad & 0.01 < M < 0.08M_\odot \\ &= Ak_1 M^{-1.3} \quad & 0.08 < M < 0.5M_\odot \\ &= Ak_2 M^{-2.3} \quad & 0.5 < M < 1M_\odot \\ &= Ak_3 M^{-2.3} \quad & 1 < M < (150M_\odot)\end{aligned}$$

- Star formation rate (SFR)
  - The SFR $\psi(t)$ gives the total mass of stars formed per unit time.
  - The mass of stars of a particular mass bin that form per unit time is then given by

$$r(M,t)dM = \psi(t)M\varphi(M)dM$$

- How to measure the SFR
  - H II regions are ionized by the integrated light of the central cluster. The ionizing radiation field is dominated by the hottest stars in the cluster. It is also possible to follow the evolution of the cluster by current theory taking into account the calculated evolution of stars within it.
  - Two limiting cases
    - **Instantaneous star formation**: the cluster is assumed to have formed in a short period. The shorter-lived high-mass stars leave the main sequence first. Thus, as the cluster ages, the radiation field corresponds to progressively cooler stars.
    - **Continuous star formation:** Massive stars that leave the main sequence are replaced with newly formed stars, while the number of long-lived low-mass stars builds up. Then, the hydrogen-ionizing radiation field does not evolve.
    - Since the emission-line spectrum of an H II region is strongly influenced by the shape of the ionizing stellar continuum, which in turn can be used to estimate the star-formation properties.

- Hα luminosity can be used as an indicator of the current star formation rate.
  - Hα luminosity gives the number of ionizing photons. For the assumed IMF, this gives the number of stars of each luminosity and spectral type.
  - O stars dies quickly, typically within 10^6 years. Therefore, their present number divided by their lifetime is their present formation rate. $\mathrm{SFR} = \dfrac{N_{\mathrm{YSO}} \langle M \rangle}{\tau}$

    Thus, the total rate of star formation can be calculated using the assumed IMF. For solar abundances and the Salpeter IMF, the SRF is

$$\begin{aligned}\mathrm{SFR}(M_\odot\,\mathrm{yr}^{-1}) &= 7.9 \times 10^{-42} L(\mathrm{H}\alpha) \quad [L(\mathrm{H}\alpha)\ \text{in erg s}^{-1}] \\ &= 1.08 \times 10^{-53} Q(\mathrm{H}^0)\ [Q(\mathrm{H}^0)\ \text{in photons s}^{-1}]\end{aligned}$$

    See https://ned.ipac.caltech.edu/level5/Sept12/Calzetti/Calzetti_contents.html
  - The same relation can be applied to any region of a galaxy. For resolved sources one can derive the SFR per unit cross section of a column along the line of sight. In unresolved cases, it is simply the total mass in stars within the object.
- The relation between mass and luminosity, the stellar evolution models, and the IMF, are all based on the assumption that observational data, derived in our Galaxy close to the sun, apply in all galaxies.
- Therefore, there are many possible errors in this chain of reasoning. In addition, an uncertain extinction correction of ionizing photons, and Hα photons must be made.

9.5 Abundances of the Elements

- Nucleosynthesis
  - First stars were formed from primordial matter, the material produced during the Big Bang.
  - This is mainly H and ^{4}He, with a small amount of D, ^{3}He, and ^{7}Li.
  - Successive generation of stars converted lighter into heavier nuclei.
  - **Primary nucleosynthesis:** the direct conversion of H into heavier elements
    - Initially, H → He. In massive stars, 3He → ^{12}C and ^{12}C + He → ^{16}O, mainly nuclei with an even number of protons, especially into those composed of α particles.
    - The production of He, C and O is quite insensitive to initial chemical composition.
    - The nuclear byproducts are returned to the ISM by a variety of mass-loss mechanisms (stellar winds, the ejection of a planetary nebula, nova outbursts, supernova explosions)
  - **Secondary nucleosynthesis:** production of elements depending on the initial abundance of their progenitors (mainly, CNO; incomplete CNO cycle, in which ^{12}C is converted into ^{14}N).
    - Later generations of stars add material to an ISM that is enriched with heavy nuclei and with the products of secondary nucleosynthesis.
- Division of the elements into three groups: X(H), Y(He), and Z(all the rest, so-called metals)
  - Abundances are specified as fractions of the total mass.
  - The ISM near the sun has $X \approx 0.7$, $Y \approx 0.28$, and $Z \approx 0.02$.
  - Z increases with time as byproducts of stellar evolution enrich the ISM.
  - Of the primordial elements, stellar processes destroy D and create ^{4}He, while ^{3}He and ^{7}Li are both created and destroyed.

- Abundance ratios
  - The abundance ratios of the primary elements, such as the C/H and O/H abundance ratios scale $\propto$ Z.
  - In the case of the secondary elements, N/C $\propto$ Z, so N/H $\propto$ Z^2.
  - However, observational results show that this picture is too simple.
- H II regions provide an important test of the theories of how stars produce the elements by nuclear processes.
  - Since the O stars which ionize the ISM are newly formed, and the composition of the ionized gas represents the current heavy-element content of the ISM.
  - For this purpose, the brighter H II regions in many external galaxies have been studied, and their spectra are quite similar to those of H II regions in our Galaxy, with the exception of the their far greater luminosity (a selection effect).
-

- Giant H II regions in other galaxies
  - **30 Doradus** (Tarantula Nebula; NGC 2070) is the nearest one, lying 50 kpc away in the LMC.
  - It is ionized by a star cluster that includes several hundred O stars, which produce $Q(\mathrm{H}^0) \sim 2 \times 10^{51}$ LyC photons per second, as deduced from the Hβ luminosity.
  - The observational results are consistent with the Salpeter IMF and a cluster age of $2-3 \times 10^6$ yr.
  - Typical electron densities, measured by [S II], are $n_e \approx 400\,\mathrm{cm}^{-3}$ for bright regions. (c.f. $n_e \leq 10^4\,\mathrm{cm}^{-3}$ in Orion Nebula).
  - Electron temperature $T_e \sim 10^4$ K, somewhat higher than in the Orion Nebula ($\approx 9{,}000$ K).
  - Diameter ~ 400 pc (100 times larger than that of the bright core of the Orion Nebula)
  - Total mass of ionized gas ~ $1010^6 M_\odot$, ~ 10^4 times larger than the Orion Nebula.
  - The velocity field is far more chaotic, in the range of 20-300 km/s, due to many supernova explosions. (The velocity field within the Orion Nebula ~ 10 km/s.)
  - These differences is probably due to the large number of evolving massive stars located within 30 Dor as well as its larger spatial scale.

- Abundance Measurements
  - Simplest method
    - (1) determine the electron temperature, derived from [O III] $\lambda 5007/\lambda 4363$ ratio.
    - (2) determine O^{++}/H^{+} ratio from [O III] $\lambda 5007/H\beta$ ratio
    - (3) determine other ionic abundances, assuming the [O III] temperature is also the same as that of the low-ionization regions that emit [O II].
    - (4) corrections for unseen stages of ionization is made, from highly schematized models, and the total elemental abundances are obtained.
  - Complex method using photoionization models of H II regions
    - The relative abundances between heavy elements are assumed to be fixed (i.e., C/O is fixed)
    - Only the abundance of heavy elements relative to H and He is varied. (C/H is varied)
    - A more sophisticated method is to allow the abundance of N (a secondary element) to vary with respect to the abundances of the "primary elements (C and O).
    - The heavy-element content in the stellar atmosphere models should be varied also to match that in the ionized gas.
    - Assumptions must be made about the dust content.
    - The luminosity distribution function and effective temperatures of the stellar model atmospheres is generally modeled by assuming an IMF and age for the cluster.

- However, [O III] λ4363 (required to determine T_e) is often too weak.
  - In this case, adopt empirical relationships between ([O II] λ3727 + [O III] $\lambda\lambda$4959,5007)/Hβ and O abundance ratios. and interpolate or extrapolate them to regions (or galaxies) where λ4363 was not observed.
  - This methods are often calibrated by reference to photoionization models.
  - A danger is that the measured heavy-element abundances in the gas may be significantly affected by depletion from the gas phase onto the dust particles.
  - This does not seem to be the major critical effect for O and Ne, while other elements (Al, Ca, and Fe) suffer major depletions, so their abundances cannot be determined.
  - The analysis results seem to confirm many of the general ideas of nucleogenesis in stars and mass return to interstellar space.
- Observed abundances in H II regions (Table 9.2)
  - The solar value comes from a mixture of photospheric and meteoric measurements and should reflect the composition of the ISM 4.5 Gyr ago, when the solar system formed.
  - The evolutionary model suggest that compositions of a nearby H II region NGC 1976 presumably reflects the ISM today. The current ISM should be more heavy-element rich than that which formed the sun.

- He abundance:
  - The most accurate determination on He abundance comes from measurements of He I and H I recombination lines in H II regions. A correction for atomic He within the H^+ zone may be needed if the star is cool.
  - Table 9.2 indicates that there are true He abundance differences among the nearby galaxies.
- Abundances of the heavy elements
  - Two approaches: (1) Strong collisionally excited lines and (2) Faint recombination lines.
  - However, for reasons that are not currently understood, the two methods disagree by factors of two or more.
- Table 9.2
  - No correction for the depletion was applied in table.

- The two methods disagree.
- There clearly are real differences in the heavy-element contents measured in H II regions in other galaxies.
- This must be related to the amount of nuclear reprocessing that has occurred over the history of the galaxy.

[Table 9.2]

Relative abundances of the elements to H, by number

Galaxy	He	C	N	O	Ne	S
Sun	0.085	2.5×10^{-4}	8.5×10^{-5}	4.9×10^{-4}	1.0×10^{-4}	1.8×10^{-5}
I Zw 18	0.078	3.5×10^{-6}	4.1×10^{-7}	1.5×10^{-5}		3.1×10^{-7}
30 Dor (coll)	0.087	6.3×10^{-5}	1.1×10^{-5}	2.1×10^{-4}	4.5×10^{-5}	6.9×10^{-6}
30 Dor (rec)	0.085	1.1×10^{-4}	1.6×10^{-5}	3.5×10^{-4}	6.8×10^{-5}	9.8×10^{-6}
NGC 1976 (coll)	0.101	2.0×10^{-4}	5.2×10^{-5}	3.1×10^{-4}	4.0×10^{-5}	9.4×10^{-6}
NGC 1976 (rec)	0.098	2.5×10^{-4}	6.0×10^{-5}	4.4×10^{-4}	7.8×10^{-5}	1.5×10^{-5}
H1013 (in M 101)	0.110		5.2×10^{-5}	5.1×10^{-4}	6.1×10^{-5}	1.2×10^{-5}

- There is a correlation of He abundance with the abundances of O, N, and Ne.
  - This indicates that nuclear burning in stars followed by return of the processed material to interstellar gas has enriched the He and heavy elements in a proportional way.

    $$Y = Y_0 + \frac{dY}{dZ} Z$$

    where Y_0 is the primordial He abundance (the mass fraction of He produced in the Big Bang), dY/dZ is proportional to the production of He and heavy elements by evolving stars.
  - These measurements thus provide an opportunity for measuring the initial production of He in the Big Bang and studying the integrated effects of stellar evolution in galaxies.

- Abundance gradients
  - In nearby galaxies, particularly in Sc galaxies,
    - [O III] ($\lambda 4959 + \lambda 5007$)/H$\beta$ increase outward.
    - [N II] ($\lambda 6548 + \lambda 6583$)/H$\alpha$ decreases outward.
    - T_e (determined from [O III] ($\lambda 4959 + \lambda 5007$)/$\lambda 4363$) is increase outward.
  - These results indicate that O/H and N/H both decrease outward.
    - O is the most abundant and the most significant coolant. Thus, its abundance decrease causes the outward increases of the temperature in the H II regions. This leads to the outward increase of [O III] ($\lambda 4959 + \lambda 5007$).
    - These effects are further influenced by the fact that the ionizing radiation field grows softer as the heavy-element abundances increase (due to their increased opacity of LyC).
  - Our Galaxy
    - Observations using the radio-frequency recombination lines (optical observations for distant H II regions are not available) shows the same radial trends as in other spiral galaxies.

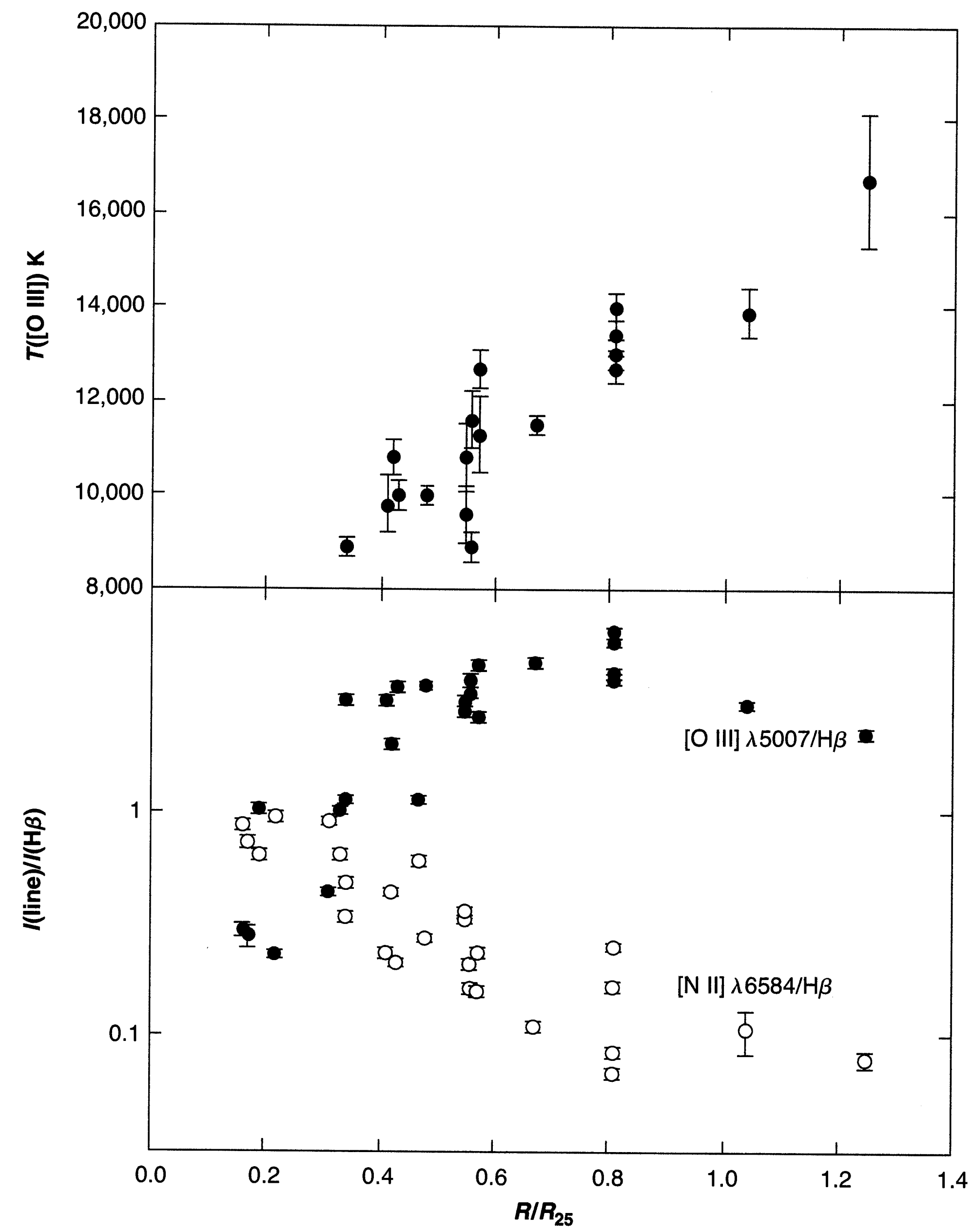

[Figure 9.5] Results obtained in M101. R_{25} represents the distance where the galaxy surface brightness falls to 25 magnitudes per square arcsec.

- No H II regions have been found with heavy-element abundances significantly larger than those of the sun.
  - This is surprising since the solar composition must reflect that of the ISM when the solar system formed ~ 5 Gyr ago.
  - (1) The continuous enrichment of the heavy elements and (2) the trends for abundances to increase towards the center of a galaxy would suggest that H II regions with a composition significantly greater than the sun should be found.
  - In these H II regions with such high heavy-element abundances, T_e would be below 10^3 K. The optical spectrum would consist solely of H I and He I recombination lines. Surveys should be able to detect such recombination-line-only nebulae. But, it is not understood why they are not observed.
- Low-luminosity irregular galaxy I Zw 18
  - The galaxy has the lowest He and heavy-element abundances.
  - Objects with zero heavy-element content would give the primordial He abundance (produced in the early universe before any star formation, recycling to interstellar gas has occurred.)
  - No such objects have been observed to date, though I Zw 18 is a close approximation to them.
  - **The easiest element to measure the abundance is O, because it is not strongly depleted from the gas.**
  - Extrapolating the correlation between Y and O/H to zero O abundance gives a primordial abundance ratio He/H = 0.077 by number or $Y_0 = 0.235$, which is consistent with the theoretical models of the Big Bang neuclpsynthesis ($0.225 < Y_0 < 0.255$, depending on the assumed photon to baryon ratio)

- The total amount of ionized gas
  - This is done directly done from measurements of the radio-frequency continuum.
  - Measurements are made at two well-separated frequencies, at both of which the Galaxy is optically thin.
  - The free-free surface brightness gives the brightness temperature

$$T_{b\nu} = 8.24 \times 10^{-2} T^{-0.25} \nu^{-2.1} \int n_+ n_e ds$$

    The measurement of $T_{b\nu}$ allows the integral to be determined. This gives the mean-square ion density (if the mean effective length is defined by a galactic model).

    The integral is proportional to the number of recombinations and hence to the number of ionization processes. It gives directly the number ionizing photons absorbed in H II regions.

    To derive the amount of ionized gas requires an estimate of its distribution along the ray (clumpiness or filling factor).

  - Observations indicate a total mass of ionized gas in the galactic plane is $\approx 4 \times 10^7 \, M_\odot$.

    Note that the total amount of gas determined from 21 cm H I observations is $\sim 5 \times 10^9 \, M_\odot$.

    The mass of the Galaxy out to 20 kpc radius is $\sim 2 \times 10^{11} \, M_\odot$.

    The total mass of the Galaxy out to ~ 200 kpc is $\sim 1.29 \times 10^{12} \, M_\odot$ (Grand et al. 2019, MNRAS Letters 487, L72).

9.6 Newly Formed Stars in H II Regions

- Star formation in dense cores of giant molecular cloud.
  - Stars must have formed from interstellar matter, and observational evidence shows that a high density of interstellar matter is strongly correlate with star formation.
  - Radio observations have lead to the discovery of many small, dense, "compact H II regions" which $n_e \approx 10^4\,\mathrm{cm}^{-3}$, nebulae that are optically invisible because of high extinction.
  - Once a condensation has reached sufficiently high density to be self-gravitating, it contracts, heating up and radiating photons by drawing on the gravitational energy source.
  - Once the star becomes hot enough at its center for nuclear reactions to begin, it quickly stabilizes on the main sequence.
  - Nebulae form as a result of density increases and star formation rapidly begins in the resulting high-density condensations.
- Evolution of H II regions
  - After the O star or stars stabilize on the main sequence, an R-type ionization front rapidly runs out into gas at a rate determined by the rate of emission of ionizing photons by the star(s).
  - Ultimately, the velocity of the ionization front reaches the R-critical velocity, and at this stage the front becomes D-critical and a shock wave breaks off and runs ahead of it, compressing the gas.
  - The nebula continues to expand and may develop a central local density minimum as a result of radiation pressure exerted on the dust particles in the nebula, or of the ram pressure of stellar winds.

- The O stars exhausts its nuclear energy sources and becomes a supernova.
- The result is the network of expanding structures, as observed in 30 Dor.
- The expansion has drawn kinetic energy from the radiation field of the star, and this kinetic energy is ultimately shared with the surrounding interstellar gas.

• T Tauri stars
  - are an example of newly forming lower-luminosity stars. Many examples have been found in nearby H II regions.
  - These are pre-main-sequence G and K stars that vary irregularly in light and have H and Ca II emission lines.
  - They are thought to be surrounded by disks of gas and dust that may be forming solar systems like our own.
  -

9.7 Starburst Galaxies

- In a normal galaxy,
  - stars form at a rate that is consistent with the cycle of stellar birth, evolution, and death, with mass return into the ISM making further star formation possible.
  - Although gas is slowly lost due to the formation of white dwarfs, neutron stars, and black holes, the current rate of star formation within our Galaxy can be sustained for a time that is comparable to its age.
- Starburst galaxies
  - are the class of galaxies in which emission lines, radiation from hot dust grains, and in the UV, continuum emission from newly formed hot stars, dominate the total emission (including stellar radiation).
  - Star formation is occurring at a greatly enhanced rate, a rate so rapid that it cannot be sustained for very long before most of the interstellar gas is used up.
  - Within our Galaxy, star formation is associated with the passage of a density wave associated with the spiral arms. The enhanced density allows the gas to become self-gravitating and undergo collapse to form stars.
  - In a starburst galaxy, the process has been greatly enhanced, often due to a merger with another galaxy, or perhaps due to the presence of an active galactic nucleus. The result is that a large number of newly-formed massive stars deposit energy into the ISM both as ionizing radiation and as mechanical energy due to stellar winds and supernova explosions.
  - **LIRG (luminous IR galaxy):** Space-based IR observatories discovered galaxies in which so much interstellar matter is present that grains absorb most of the UV and optical radiation (in 1983 with IRAS). LIRGs are galaxies with luminosities above $10^{11} L_\odot$. Very little optical or UV radiation escapes from the ultraluminous infrared galaxies because nearly all of the star light is reprocessed into dust emission.

[Nuclear Burning]

- The power source for most stars is the burning of hydrogen in the core of the star.
  - The pressures and temperatures there are sufficient to allow the hydrogen nuclei to undergo fusion reactions that lead to helium. (The core temperature of the sun is 1.6×10^6 K.)
  - Such reactions are exothermic. They release energy in the form of kinetic energy of the reaction productions. The result is that the star remains in a fairly stable state for much of its active life — some 10^{10} yr in the case of the sun.
- **Stable equilibrium** (is maintained by a negative feedback mechanism.)
  - It the star is perturbed to smaller size, the densities and temperatures increase owing to the greater gravitational force. This leads to more nuclear reactions. The increased energy output into the core causes the star to expand, thus returning it to its original state.
  - If the star is perturbed to a larger size, the reduced densities and temperatures diminish the energy output, and the star will shrink back to its original stable state.
- **Nuclear Warmer**
  - Only a tiny fraction of the stellar thermal energy of a star is radiated away from the stellar surface — only $\sim 5 \times 10^{-8}$ for the sun. The nuclear energy that must be supplied to compensate this loss is thus only a very small fraction of the total thermal energy of the sun.
  - Therefore, the sun is not like a raging nuclear furnace but a huge ball of hot gas with a low-powered nuclear “warmer.” In other words, the sun is a very big house with high thermal content.
  - A basic model of a normal star can thus treat the star simply as a gravitationally bound, stable ball of hot gas.

Quantum Tunneling

- **Coulomb Barrier & Tunneling**
  - The dominant element in the sun is hydrogen, and it is completely ionized throughout most of the solar volume.
  - For proton-proton interactions to take place, the protons must come within the short range of the nuclear forces, and their kinetic energies should be great enough to overcome the huge Coulomb repulsion force at these short distances. However, the average kinetic energy of protons at the core of the sun is ~ 1000 less than required.
  - This problem is surmounted by the wave nature of particles that allows them to penetrate some distance into potential barriers. If the barrier is sufficiently narrow, a particle can leak through it into the nuclear potential well. There are sufficient numbers of particles in the high-energy tail of the Maxwell-Boltzmann distribution at 10^7 K to provide the required leakage into the nuclear well and hence nuclear reactions. The reaction rates are highly temperature sensitive. A modest temperature rise markedly increase the rate of nuclear interactions.

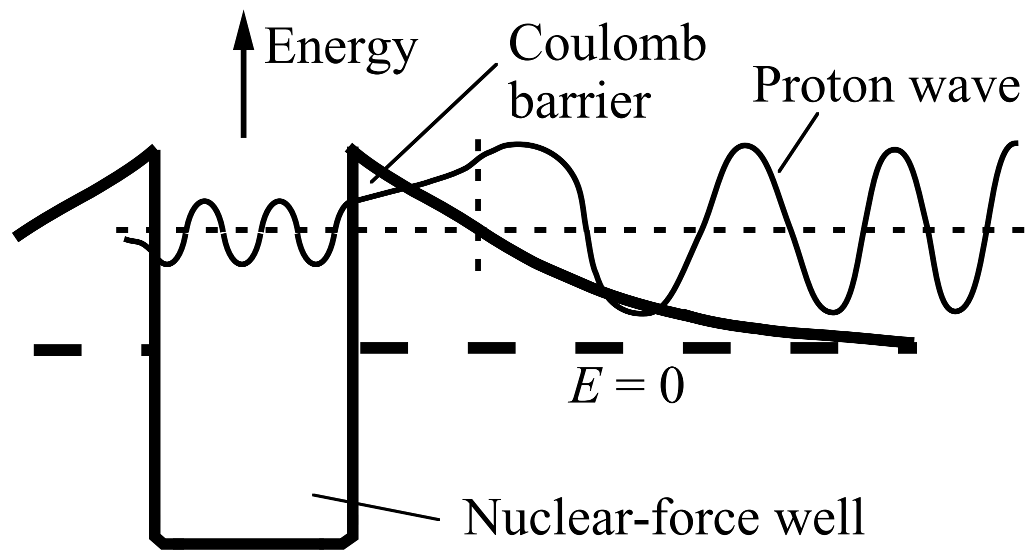

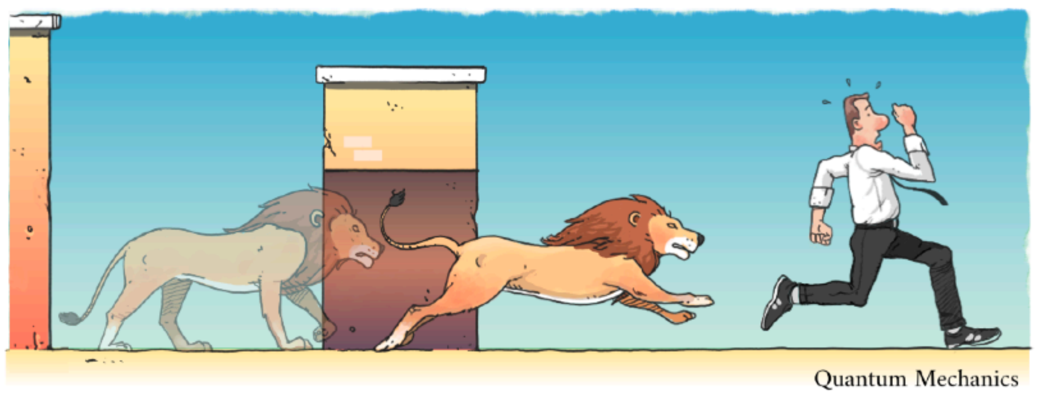

credit: LibreTexts, Chemistry

Burning Shells: Onion-like structure

- Above a certain mass ($M_* \gtrsim 10 M_\odot$), stars are able to fuse elements up to iron. (The exact value of this mass is not known with precision.)

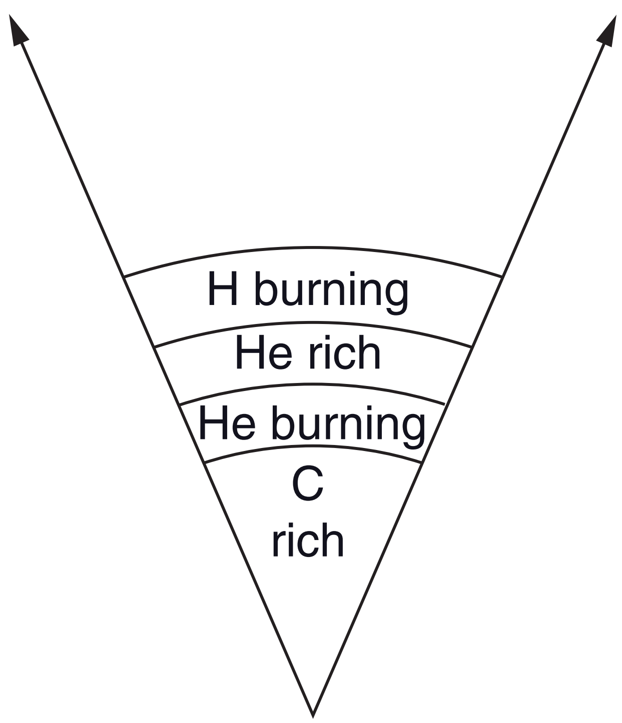

Illustration of the central region of 1 $M_\odot$ star near the end of its nuclear-burinig life.

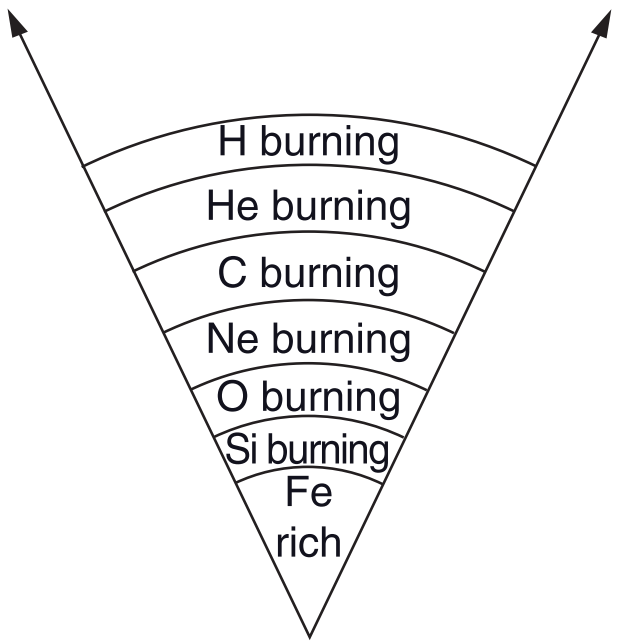

Onion-like structure of a massive star ($M_* \gtrsim 10 M_\odot$) near the end of its life.

[Helium] Proton-proton (pp) chain

- The dominant chain of nuclear interactions in the sun is the proton-proton (pp) chain.
  - The pp chain can take place at temperatures above 5×10^6 K.
  - The series of reactions in this chain **coverts four protons to a helium nucleus** (two protons + two neutrons). The latter is referred to as an ***alpha particle***.

PPI chain

$$
\begin{aligned}
{}^1\mathrm{H} + {}^1\mathrm{H} &\to {}^2\mathrm{H} + e^+ + \nu_e \\
{}^1\mathrm{H} + {}^1\mathrm{H} &\to {}^2\mathrm{H} + e^+ + \nu_e \\
{}^1\mathrm{H} + {}^2\mathrm{H} &\to {}^3\mathrm{He} + \gamma \\
{}^1\mathrm{H} + {}^2\mathrm{H} &\to {}^3\mathrm{He} + \gamma \\
{}^3\mathrm{He} + {}^3\mathrm{He} &\to {}^4\mathrm{He} + 2\,{}^1\mathrm{H}
\end{aligned}
$$

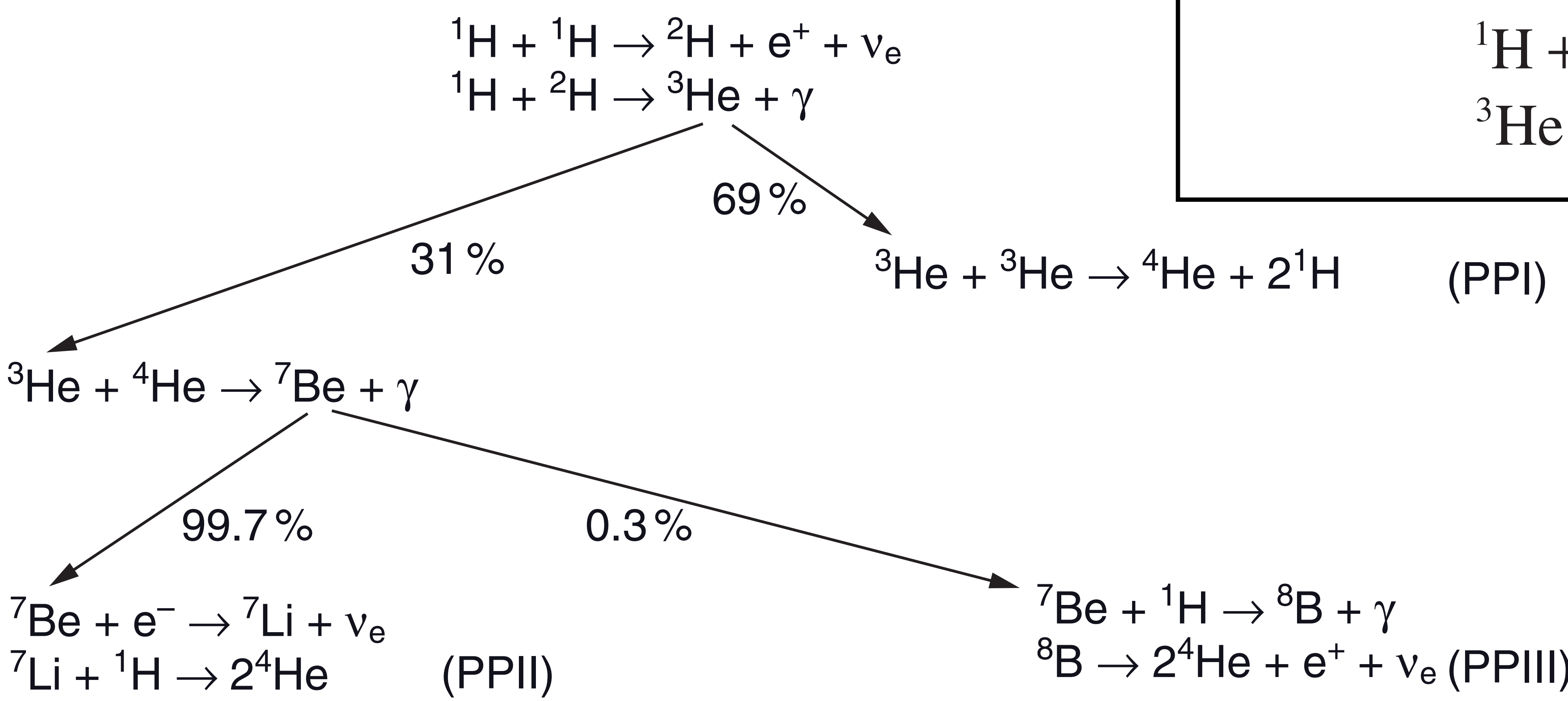

atomic numbers
Li: $Z = 3$
Be: $Z = 4$
B: $Z = 5$

[Helium] CNO Cycles

- The CNO cycles are made up of reactions in which **protons are fused with C, N and O nuclei to produce helium.**
- The CNO process makes use of the occasional carbon nucleus in the core of a star that was formed from the debris of previous generations of stars.
- The CNO cycles dominate energy generation in main-sequence stars only for masses larger than 1.5 $M_\odot$.

CNOI	CNOII	CNOIII
${}^{1}\mathrm{H} + {}^{12}\mathrm{C} \rightarrow {}^{13}\mathrm{N} + \gamma$		
${}^{13}\mathrm{N} \rightarrow {}^{13}\mathrm{C} + e^{+} + \nu_e$		
${}^{1}\mathrm{H} + {}^{13}\mathrm{C} \rightarrow {}^{14}\mathrm{N} + \gamma$		
${}^{1}\mathrm{H} + {}^{14}\mathrm{N} \rightarrow {}^{15}\mathrm{O} + \gamma \longrightarrow$	${}^{1}\mathrm{H} + {}^{14}\mathrm{N} \rightarrow {}^{15}\mathrm{O} + \gamma$	
${}^{15}\mathrm{O} \rightarrow {}^{15}\mathrm{N} + e^{+} + \nu_e \longrightarrow$	${}^{15}\mathrm{O} \rightarrow {}^{15}\mathrm{N} + e^{+} + \nu_e$	
${}^{1}\mathrm{H} + {}^{15}\mathrm{N} \rightarrow {}^{12}\mathrm{C} + {}^{4}\mathrm{He}$	${}^{1}\mathrm{H} + {}^{15}\mathrm{N} \rightarrow {}^{16}\mathrm{O} + \gamma \longrightarrow$	${}^{1}\mathrm{H} + {}^{15}\mathrm{N} \rightarrow {}^{16}\mathrm{O} + \gamma$
	${}^{1}\mathrm{H} + {}^{16}\mathrm{O} \rightarrow {}^{17}\mathrm{F} + \gamma \longrightarrow$	${}^{1}\mathrm{H} + {}^{16}\mathrm{O} \rightarrow {}^{17}\mathrm{F} + \gamma$
	${}^{17}\mathrm{F} \rightarrow {}^{17}\mathrm{O} + e^{+} + \nu_e \longrightarrow$	${}^{17}\mathrm{F} \rightarrow {}^{17}\mathrm{O} + e^{+} + \nu_e$
	${}^{1}\mathrm{H} + {}^{17}\mathrm{O} \rightarrow {}^{14}\mathrm{N} + {}^{4}\mathrm{He}$	${}^{1}\mathrm{H} + {}^{17}\mathrm{O} \rightarrow {}^{18}\mathrm{F} + \gamma$
		${}^{18}\mathrm{F} \rightarrow {}^{18}\mathrm{O} + e^{+} + \nu_e$
		${}^{1}\mathrm{H} + {}^{18}\mathrm{O} \rightarrow {}^{15}\mathrm{N} + {}^{4}\mathrm{He}$

atomic numbers
C: Z = 6
N: Z = 7
O: Z = 8
F: Z = 9

[Carbon] Helium-Burning Phase - Triple-α process

- During the hydrogen-burning phase, 4 protons are transformed into ^{4}He nuclei and therefore the composition of the core gradually changes.
  - This process leads to an increase to the mean molecular weight in the stellar core.
  - An increase of the mean molecular weight leads to a decrease of gas pressure. The core progressively contracts during the core hydrogen-burning phase thereby increasing the density and temperature (and pressure).
  - If the mass of the star is larger than 0.5 $M_\odot$, the core will, following its contraction, attain the critical temperature ($\approx 10^8$ K) needed for the fusion of helium.
  - Helium in the core of the evolved star can burn via the following chain of reactions:

$$
\begin{aligned}
&^4\mathrm{He} + {}^4\mathrm{He} \rightarrow {}^8\mathrm{Be} + \gamma \\
&^8\mathrm{Be} + {}^4\mathrm{He} \rightarrow {}^{12}\mathrm{C}^* + \gamma \\
&^{12}\mathrm{C}^* \rightarrow {}^{12}\mathrm{C} + \gamma
\end{aligned}
$$

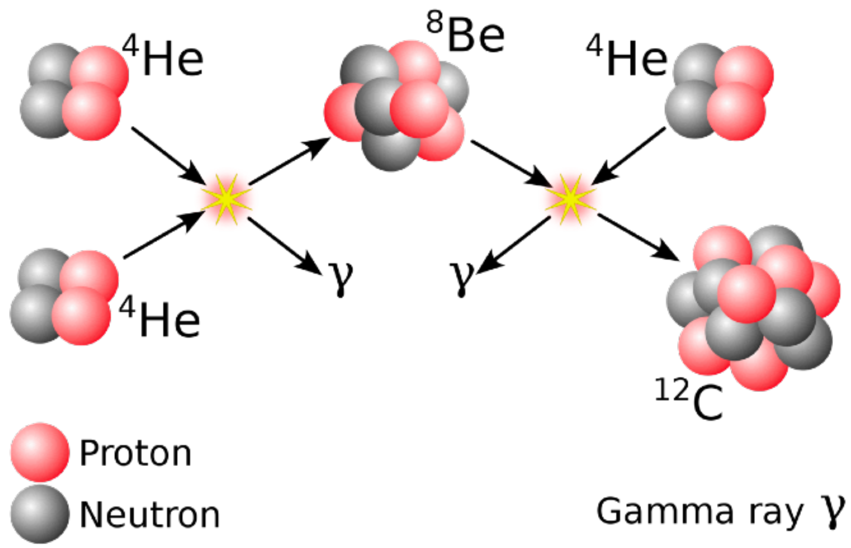

[wikipedia]

  - This chain is commonly called the triple-α reaction since the three α particles fuse to create a carbon nucleus.

Alpha process elements

- Alpha process elements (or α elements) are so-called since their most abundant isotopes are integer multiples of four - the mass of the helium nucleus (the α particle).
  - The stable alpha elements are C, O, Ne, Mg, Si, and S.
  - The alpha process generally occurs only if the star is sufficiently massive ($\gtrsim 10 M_\odot$). These stars contract as they age, increasing core temperature and density to high enough levels to enable the alpha process.
  - Requirements increase with atomic mass, especially in later stages — sometimes referred to as silicon burning — and thus most commonly occur in supernovae.
  - **Type II supernovae mainly synthesize oxygen and the α-elements** (Ne, Mg, Si, S, Ar, Ca, and Ti) while **Type Ia supernovae mainly produce elements of the iron peak** (Ti, V, Cr, Mn, Fe, Co, and Ni). An iron peak element is an element with an atomic number in the vicinity of iron's (26).
  - The abundance of total α elements in stars is usually expressed in terms of logarithms:

$$\left[\frac{\alpha}{\mathrm{Fe}}\right] \equiv \log_{10}\left(\frac{N_{\mathrm{E}\alpha}}{N_{\mathrm{Fe}}}\right)_{\mathsf{Star}} - \log_{10}\left(\frac{N_{\mathrm{E}\alpha}}{N_{\mathrm{Fe}}}\right)_{\mathsf{Sun}},$$

  - The relative abundances of the two groups reveal information of past supernovae and star formation history.

Burning Phases

- Carbon burning leads to the creation of oxygen, neon and magnesium.
  - $^{12}C + {}^{4}He \rightarrow {}^{16}O + \gamma$
  - $^{12}C + {}^{12}C \rightarrow {}^{20}Ne + {}^{4}He$
  - $^{12}C + {}^{12}C \rightarrow {}^{24}Mg + \gamma$
- Neon burning:
  - It would be natural that the next phase of nuclear burning would be fusion reactions related to oxygen. However, the critical temperature for neon fusion with α particles is lower than for oxygen burning. At the high temperatures, a sufficient number of energetic photons are present that can lead to photodisintegration of a portion of the neon nuclei
  - $^{20}Ne + \gamma \rightarrow {}^{16}O + {}^{4}He$
  - This photodisintegration reactions create α particles that can then react with the remaining neon via the reactions
  - $^{20}Ne + {}^{4}He \rightarrow {}^{24}Mg + \gamma$
  - $^{24}Mg + {}^{4}He \rightarrow {}^{28}Si + \gamma$
  - $^{20}Ne + {}^{20}Ne \rightarrow {}^{16}O + {}^{24}Mg$

- The iron peak is a local maximum in the vicinity of Fe (Cr, Mn, Fe, Co and Ni) on the plot of the abundances of the chemical elements.

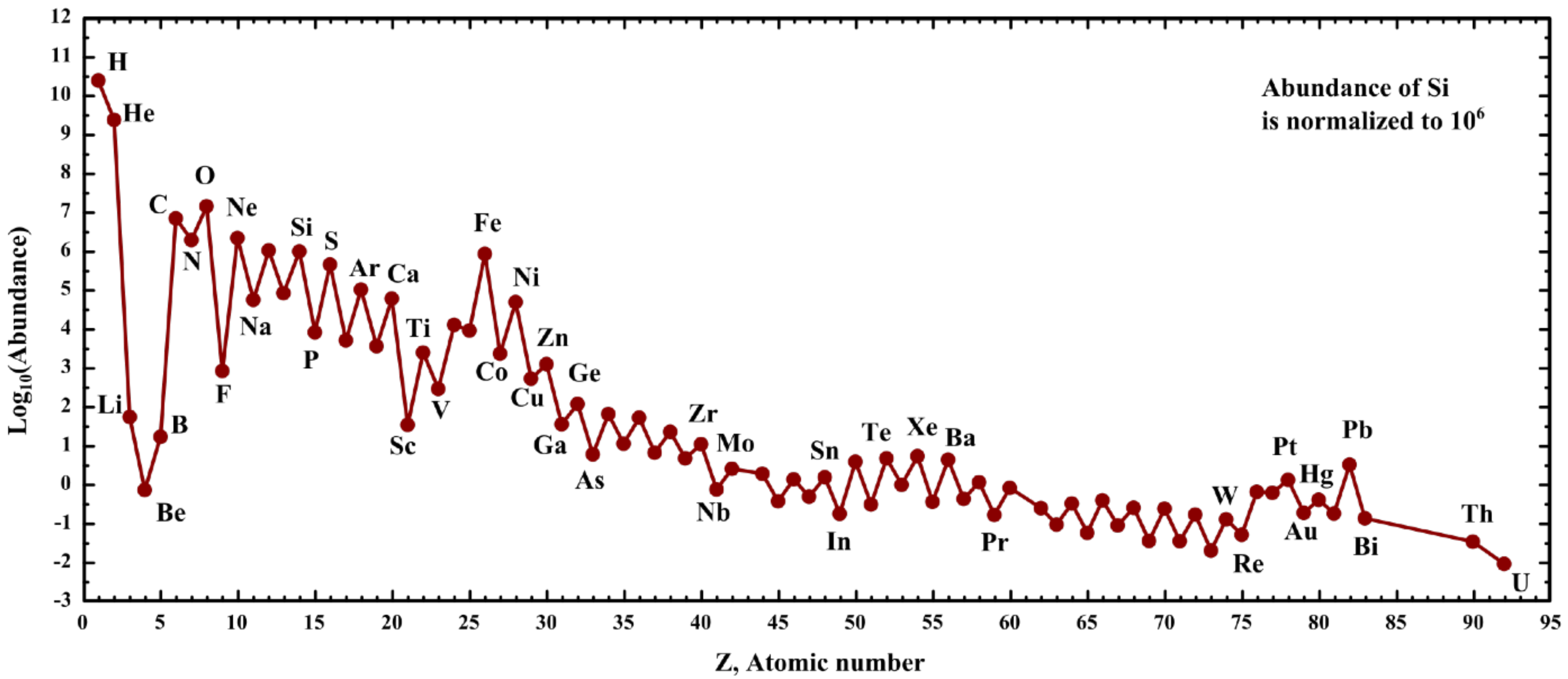

wikipedia

Burning phase	Elements produced	Central temperature	Timescale
H	He	6.0×10^7 K	7×10^6 yr
He	C, O	2.0×10^8 K	5×10^5 yr
C	O, Ne, Mg	9.0×10^8 K	600 yr
Ne	O, Mg, Si	1.7×10^9 K	0.5 yr
O	Si, S	2.3×10^9 K	6 d
Si	Fe-peak	4.0×10^9 K	1 d

https://www.chem.ualberta.ca/~massspec/atomic_mass_abund.pdf